PFC/JA-87-23

Particle Transport Simulation of Density Behavior During Lower-Hybrid Current Drive Experiments On the Versator II Tokamak

K-I. Chen, S.C. Luckhardt, M.J. Mayberry,* M. Porkolab

May 1987

Plasma Fusion Center
Massachusetts Institute of Technology
Cambridge, Massachusetts 02139 USA

This work was supported by DOE Contract No. DE-AC02-78ET-51013.

Submitted for publication to Nuclear Fusion

*Present address: GA Technologies Inc., San Diago, CA 92318

PARTICLE TRANSPORT SIMULATION OF DENSITY BEHAVIOR DURING LOWER-HYBRID CURRENT DRIVE EXPERIMENTS ON THE VERSATOR II TOKAMAK

K-I. Chen, S.C. Luckhardt, M.J. Mayberry,* M. Porkolab

Plasma Fusion Center and Research Laboratory of Electronics

Massachusetts Institute of Technology

Cambridge, Massachusetts 02139

ABSTRACT

Previous analysis of the global particle balance has shown that significant density increases observed in Versator II with both 800MHz and 2.45GHz lower-hybrid current drive experiments are the result of an improvement by a factor of two in the particle confinement time. In the present work the one-dimensional particle transport equation has been solved numerically to simulate temporal and spatial evolution of the electron density. In order to fit the 800MHz profiles, it is found that the main contribution to the profile change is due to a severalfold increase of the inward pinch velocity. However, for the 2.45GHz data case, a reduction of the diffusive term near the periphery seems to be needed to explain the observed profiles.

1. INTRODUCTION

Understanding particle transport in tokamaks is an important physics issue as it relates to density control, fueling, etc. Previous studies of particle transport have been performed predominantely in ohmically heated discharges [1-4]. The main result from those studies is that besides an outward diffusive particle flux, an inward particle flux is needed to explain the observed density profiles. Furthermore, both transport coefficients (diffusion coefficient D and inward pinch velocity v) are 10-100 larger than the values predicted by the neoclassical theory.

The energy transpot during discharges with the application of auxiliary heating has been addressed before [5,6]; however, the particle transport under the influence of auxiliary heating power has not been studied as extensively. In this paper, the particle transport during lower-hybrid current drive (LHCD) experiments on the Versator II tokamak will be analyzed. Details of the Versator II tokamak and RF experiments have been described elsewhere [7].

In earlier experiments [8,9,10], it has been shown that the significant density increases observed in both Versator 800MHz and 2.45GHz LHCD experiments are due to a factor of two improvement in particle confinement time. Furthermore, the particle confinement improvement only occurs in the RF current drive regime. The purpose of this paper is to model the density profiles obtained in the experiment with a particle transport code and obtain values for the spatial diffusion coefficient D and the inward pinch velocity v.

2. MODEL SIMULATION

The one-dimensional particle transport equation [2] is

$$\frac{\partial n_e(r,t)}{\partial t} = \frac{1}{r}\frac{\partial}{\partial r}\left[r\left[D\frac{\partial}{\partial r} + v\right] n_e(r,t)\right] + S(r,t) \qquad (1)$$

where $n_e(r,t)$ is the local electron density, D is the diffusion coefficient, v is the pinch velocity and $S(r,t)$ is the electron source term which is mainly due to ionization of hydrogen neutrals. The traditional way to simulate particle transport problem is to convert the above parabolic differential equation into a difference equation with the assumption that n_e and $S(r,t)$ are known. Model simulated profiles obtained through different trial values of D's and v's are compared with experimentally obtained profiles. Then D and v are determined by the best fit of the profile. In the present case, $n_e(r,t)$ and $S(r,t)$ are measured in the experiment. The density profiles have been obtained by Abel inversion of a twelve chord interferometry scan, and the source term $S(r,t)$ is inferred by spectroscopic measurement of the H_α profile. Equation (1) is solved numerically by the Crank-Nicolson implicit method [10]. In modeling the anomalous D and v, the simplest radial dependences have been chosen as a starting point; namely, the diffusion coefficient D is constant and the convective velocity is linearly proportional to the radius $v(r)=v_0 \cdot r/a$. This simple model has been used by other authors [2,3] and appears to be adequate to explain some of the experimental results. However, it will be necessary to introduce additional spatial variation of D to accurately model the 2.45 GHz LHCD experiments. Details of this modified model will be discussed later.

2.1. 800MHz LHCD

Figure 1 shows the temporal evolution of the line-averaged density and the density profile during 800MHz LHCD. In the absence of the RF current drive, the density profiles are relatively flat (n_{e0}(central)/$\bar{n}_e$(line average) $\sim$1.2). To model the temporal and spatial profiles in the initial ohmic phase, $D=15000 cm^2/sec$ and $v(r)=600 \cdot (r/a) cm/sec$ are found to be optimum values. The experimental profile and model simulation profiles are shown in Fig. 2(a). The source term $S(r,t)$ is represented by a Gaussian profile with an appropri-

ate width and time dependence to approximate the experimental profile. The agreement between the modeling and the experimental values for the ohmic phase is good within 4% over the entire radial profile.

During RF current drive, the density initially increases and the profile becomes more peaked ($(n_{e_0}/\bar{n}_e)_{max}\sim 1.9$) (see Fig. 1). Note the source term in Fig. 2 is decreasing during the course of the RF pulse. The steady state solution ($(\partial n/\partial t)=0$) of a source free ($S(r,t)=0$) transport equation is a Gaussian density profile with a half width proportional to (v/D). Because the source term is small or negligible near the central part of the plasma, the overall density profile shape, especially near the center, is determined by the ratio v/D. Putting this another way, the ratio v/D measures the relative importance of the inward convective flow and the outward diffusive flow. Thus, the observed peaking of the density profile, indicates that the value of v/D should be increased during RF current drive. An interesting question is whether this increase is due to the increase of v and/or the decrease of D. Figure 3 shows the results of three numerical calculations with approximately the same v/D value. Simulation #1 yields the best fit (also see Figs. 2(b-e)), with a severalfold increase in v and unchanging D value. Note that this simulation correctly predicts both the initial increase and the subsequent decrease of the electron density while the D and v are held constant. Hence, the density decrease in the later part of the RF pulse is due to the decreasing source term, not a change in transport.

Simulations #2 and #3 predict continually increasing density behavior which is not consistent with measured profiles. To test the effects of radial dependence of the transport coefficient, a more sophisticated transport model was used, specifically, the diffusion coefficient $D=D_0\cdot(1+C_1(r/a)^{C_2})$ where $3\lesssim C_1\lesssim 10$, $1.5\lesssim C_2\lesssim 4$ and the pinch velocity $v(r)=v_0\cdot(r/a)^2$ [11,12]. These models did not seem to make any improvement in the predictions relative to the results

obtained from the simpler model with D independent of r and $v \propto r$. Therefore, it appears that the density rise and confinement improvement is mainly a consequence of an increased inward particle convection during RF current drive.

After the termination of the RF pulse, the particle transport deteriorates. This is correlated with an anomalous Doppler relaxation mode burst which occurs after the RF pulse [8]. This instability manifests itself by showing bursts in most diagnostics; e.g., loop voltage, hard x-ray, H_α emission. Using the pre-RF injection values of D and v results in profiles which are in significant error ($\sim$75%) in the peripheral part of the discharge. However, if the transport model shown in Fig. 4(a) is used; i.e., the diffusive loss is larger near the outside, the predicted profiles are in considerable better agreement (10%$\sim$20%) with the experiment. Table I summarizes the parameters used in model simulations of the 800 MHz experiments.

2.2. 2.45 GHz LHCD

Figure 5 shows the temporal evolution of the line-averaged density and the profile during 2.45GHz LHCD. In the initial ohmic phase, the density profile is more peaked ($n_{e0}/\bar{n}_e \sim 2$) compared to the profile in the lower density 800MHz LHCD regime. $D=5000 cm^2/sec$ and $v(r)=2100\cdot(r/a)cm/sec$ produces a good fit to the observed ohmic heating density profiles (see Fig. 6(a)).

During the RF current drive pulse, the density increases and the profile becomes broader ($n_{e0}/\bar{n}_e \sim 1.5$). Hence, near the center the ratio v/D must decrease relative to the pre-RF values. Four representative models have been used in simulating these experiments. Following the guidelines of decreasing v/D, simulation #4 uses a model shown in Fig. 4(b), which decreases the value of v near the center by an order of magnitude and increases its value by a factor of two near the edge. This particle transport model does not successfully model the time evolution of the density. In particular, the simulation density decreased more rapidly than the experimental results. When the value of D

(simulation #2) or the value of v (simulation #3) was increased by a factor of two, the experimental profiles could not be reproduced (see Fig. 7). In both simulations, the density increased more rapidly than experiment and was more peaked than experiment. Figures 6(b-d) show the much better results obtained in simulation #1. The model of D used in simulation #1 is shown in Fig. 3(a). D was increased near the center, and decreased near the periphery. The code simulation is in much better agreement with the measured profile as shown in Fig. 6.

To model the post RF-phase, the pre-RF D and v values have been used. This model is in good agreement with the experimental profile (see Fig. 6(e)). Table II lists values of D and v used in these simulations.

3. DISCUSSION AND SUMMARY

Equation (1) can be integrated to obtain the following equation

$$\frac{1}{r'}\int_0^{r'} r\left[\frac{\partial n}{\partial t} - S\right] dr = D\frac{\partial n}{\partial r} + vn \qquad (2)$$

If for $r<r'$, $S=0$, and $(\partial n/\partial t)=0$, Eq. (2) yields

$$D\frac{\partial n}{\partial r} + vn = 0$$

Consequently, we obtain

$$\frac{v}{D} = -\frac{\partial \ell n(n)}{\partial r} \qquad (3)$$

Equation (3) implies that for a source free, steady state particle transport, the ratio v/D is determined by the scale length of the density profile. Table III shows the value of v/D from the profile measurement and from the model used to yield the best fit. The values of v/D obtained from profile measurements and best fit models are in close agreement.

Particle confinement improvement has been confirmed in both 800MHz LHCD and 2.45GHz LHCD cases which have quite different density profile shapes.

Some recent ASDEX results indicate the same trend [13,14]. It has been found in ASDEX that improved particle confinement can be achieved in H-mode of neutral beam heated plasmas which have the broader density profile, and in ohmic discharges with pellet injection which have the more peaked profile. Thus, the particle confinement under the influence of auxiliary heating or fueling does not seem to be solely dictated by the degree of the peakedness of the density profile. One caveat here is that based on the data of the ALCATOR C and FT high field, high density ohmic discharges, it has been suggested that the more peaked density profile seemed to be correlated with the better confinememt [15].

In summary the inward convective velocity was found to increase by a factor of eight to model the 800MHz experimental result of improved confinement and peaked profiles. In the 2.45GHz case, the diffusive loss had to be reduced near the plasma periphery also modeling improved confinement but with broadened profile. The difference in the particle transport in the two LHCD experiments might be related to the difference of wave penetration and current generation in the two different density and RF frequency regimes. In particular, the wave accessibility condition is more stringent for the 2.45GHz experiment. Thus, the wave absorption profile might be quite different for these two LHCD experiments. However, the physical reason for particle confinement improvement during lower-hybrid current drive experiments in Versator II is not understood at present.

ACKNOWLEDGEMENTS

One of the authors (K.C.) would like to acknowledge useful discussions with James L. Terry. This work was supported by the US Department of Energy Cont. DE-AC01-78ET-51013.

*Present address: GA Technologies Inc., San Diego, CA 92318

REFERENCES

[1] COPPI, B. and SHARKY, N., Nucl. Fusion 21, (1983) 1363.

[2] STRACHAN, J.D., et al, Cucl. Fusion 22, (1982) 1145.

[3] RICHARDS, B., et al Bull. of Am. Phys. Soc. 30 (1985) 1567.

[4] EFTHIMION, P.C., et al, Bull Am. Phys. Soc. 31 (1986) 1415.

[5] KAYE, S.M. and GOLDSTON, R., Nucl. Fusion 25 (1985) 65.

[6] TAKASE, Y., et al, Nucl. Fusion 27 (1987) 53.

[7] LUCKHARDT, S.C., et al, Phys. Rev. Lett. 48 (1982) 152.

[8] LUCKHARDT, S.C., et al, Phys. Fluids 29 (1986) 1985

[9] MAYBERRY, M.J., CHEN, K.I., LUCKHARDT, S.C., PORKOLAB, M., (to be published in Physics of Fluids).

[10] MITCHELL, A.R., GRIFFITHS, D.F., "The Finite Difference Method in Partial Differential Equations", New York, Wiley (1980).

[11] FURTH, H.P., in "Fusion", edited by E. TELLER, New York, Academic Press, 1981, p. 203.

[12] BECKER, G., Nucl. Fusion 27 (1987) 11.

[13] SINGER, C.E., et al, Nucl. Fusion 25 (1985) 1555.

[14] VLASES, G., et al, Nucl. Fusion 27 (1987) 351.

[15] High Field Tokamak Workshop, Boston, June 1981 (unpublished).

FIGURE AND TABLE CAPTIONS

Fig. 1. The temporal evolution of the line-averaged density and the density profile during 800MHz LHCD.

Fig. 2. Model simulation #1 of 800MHz LHCD; (a) before the RF (b), (c), and (d) during the RF and (e) after the RF.

Fig. 3. Three-model simulations of the density evolution on 800MHz LHCD at various radii.

Fig. 4. Modified transport model of (a) diffusion coefficient and (b) pinch velocity.

Fig. 5. The temporal evolution of the line-averaged density and the density profile during 2.45GHz LHCD.

Fig. 6. Model simulation #1 of 2.45GHz LHCD: (a) before the RF, (b), (c), and (d) during the RF and (e) after the RF.

Fig. 7. Four-model simulations of the density evolution on 2.45GHz LHCD at various radii.

Table I. Transport parameters used on model simulations of 800MHz LHCD

Table II. Transport parameters used on model simulations of 2.45GHz LHCD.

Table III. The ratio of pinch velocity (v) and diffusion coefficient (D) from experimental density profiles and from model simulations.

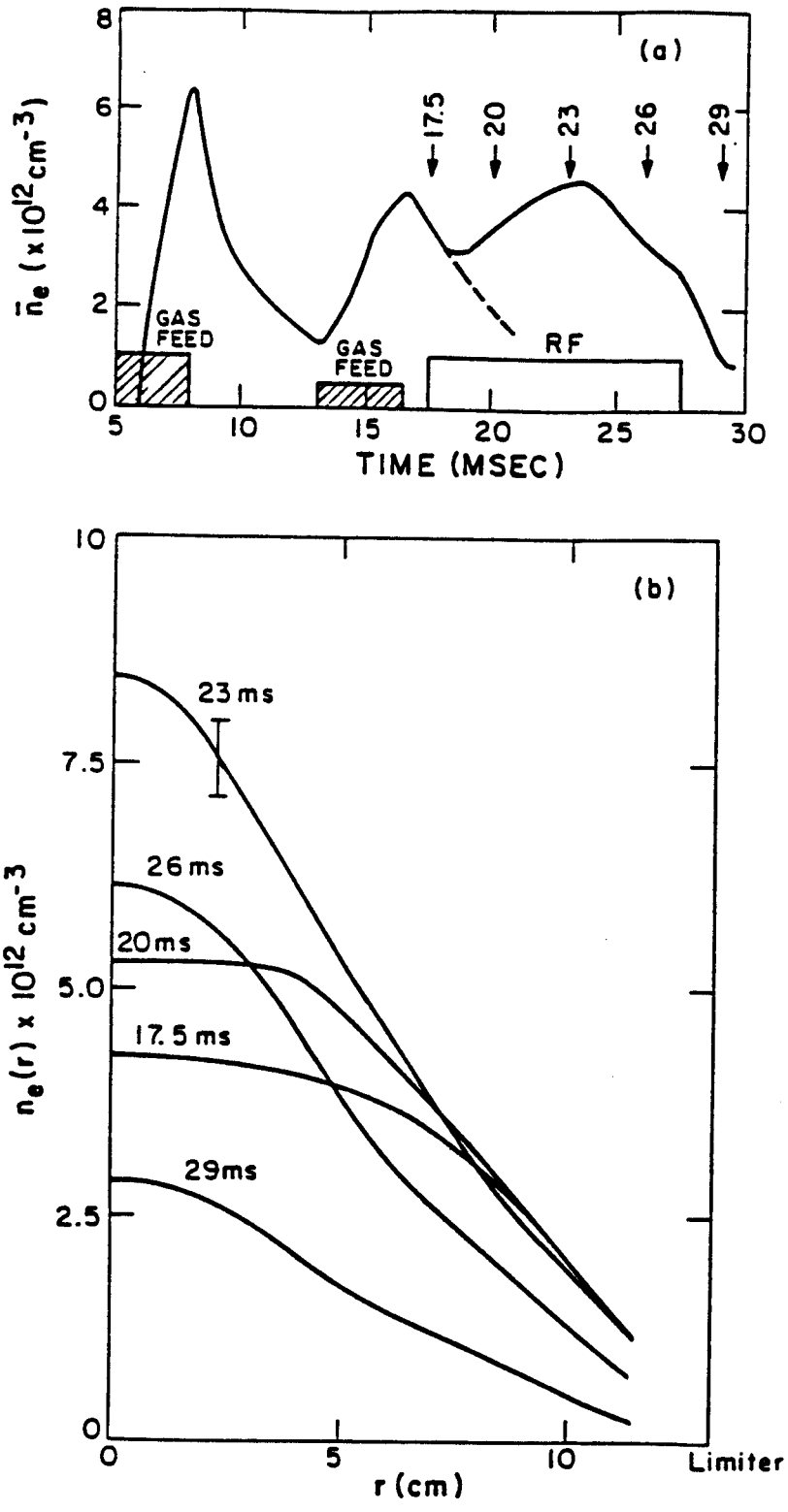
(a)
$\bar{n}_e$ ($\times 10^{12}$cm^{-3})
8
6
4
2
0
17.5
20
23
26
29
GAS FEED
GAS FEED
RF
5
10
15
20
25
30
TIME (MSEC)
(b)
$n_e(r) \times 10^{12}$ cm^{-3}
10
7.5
5.0
2.5
0
23 ms
26 ms
20 ms
17.5 ms
29 ms
0
5
10
Limiter
r (cm)

Fig. 1

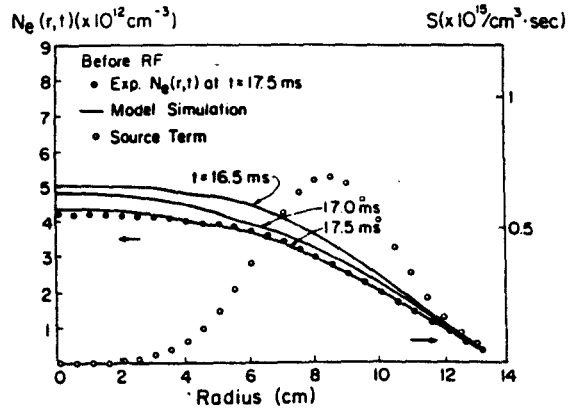
N_e (r,t)(x10^{12}cm^{-3})
S(x10^{15}/cm^3·sec)
Before RF
• Exp. N_e(r,t) at t=17.5 ms
— Model Simulation
• Source Term
t=16.5 ms
17.0 ms
17.5 ms
Radius (cm)

(a)

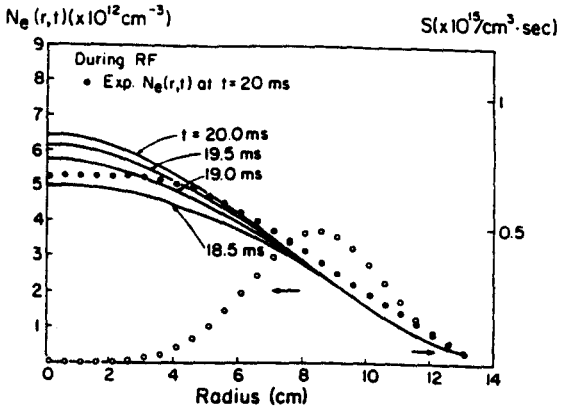
N_e (r,t)(x10^{12}cm^{-3})
S(x10^{15}/cm^3·sec)
During RF
• Exp. N_e(r,t) at t=20 ms
t=20.0 ms
19.5 ms
19.0 ms
18.5 ms
Radius (cm)

(b)

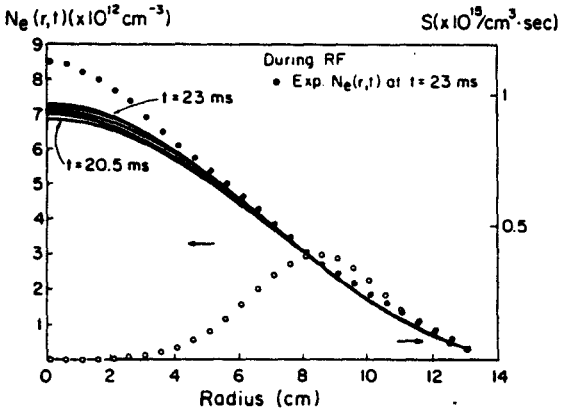
N_e (r,t)(x10^{12}cm^{-3})
S(x10^{15}/cm^3·sec)
During RF
• Exp. N_e(r,t) at t=23 ms
t=23 ms
t=20.5 ms
Radius (cm)

(c)

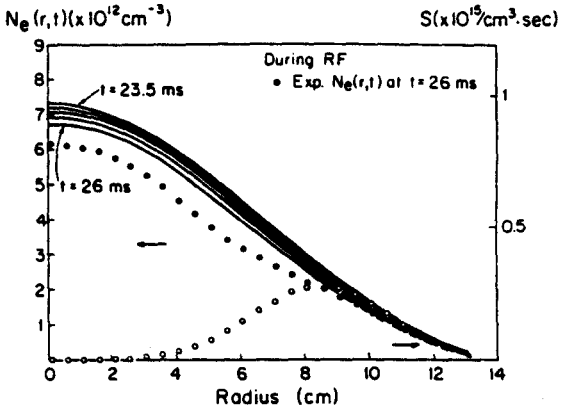
N_e (r,t)(x10^{12}cm^{-3})
S(x10^{15}/cm^3·sec)
During RF
• Exp. N_e(r,t) at t=26 ms
t=23.5 ms
t=26 ms
Radius (cm)

(d)

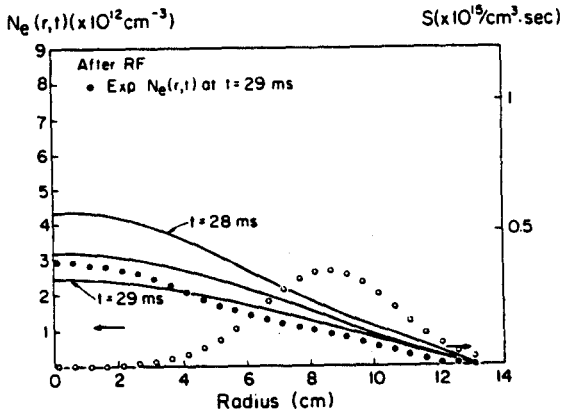
N_e (r,t)(x10^{12}cm^{-3})
S(x10^{15}/cm^3·sec)
After RF
• Exp. N_e(r,t) at t=29 ms
t=28 ms
t=29 ms
Radius (cm)

(e)

Fig. 2

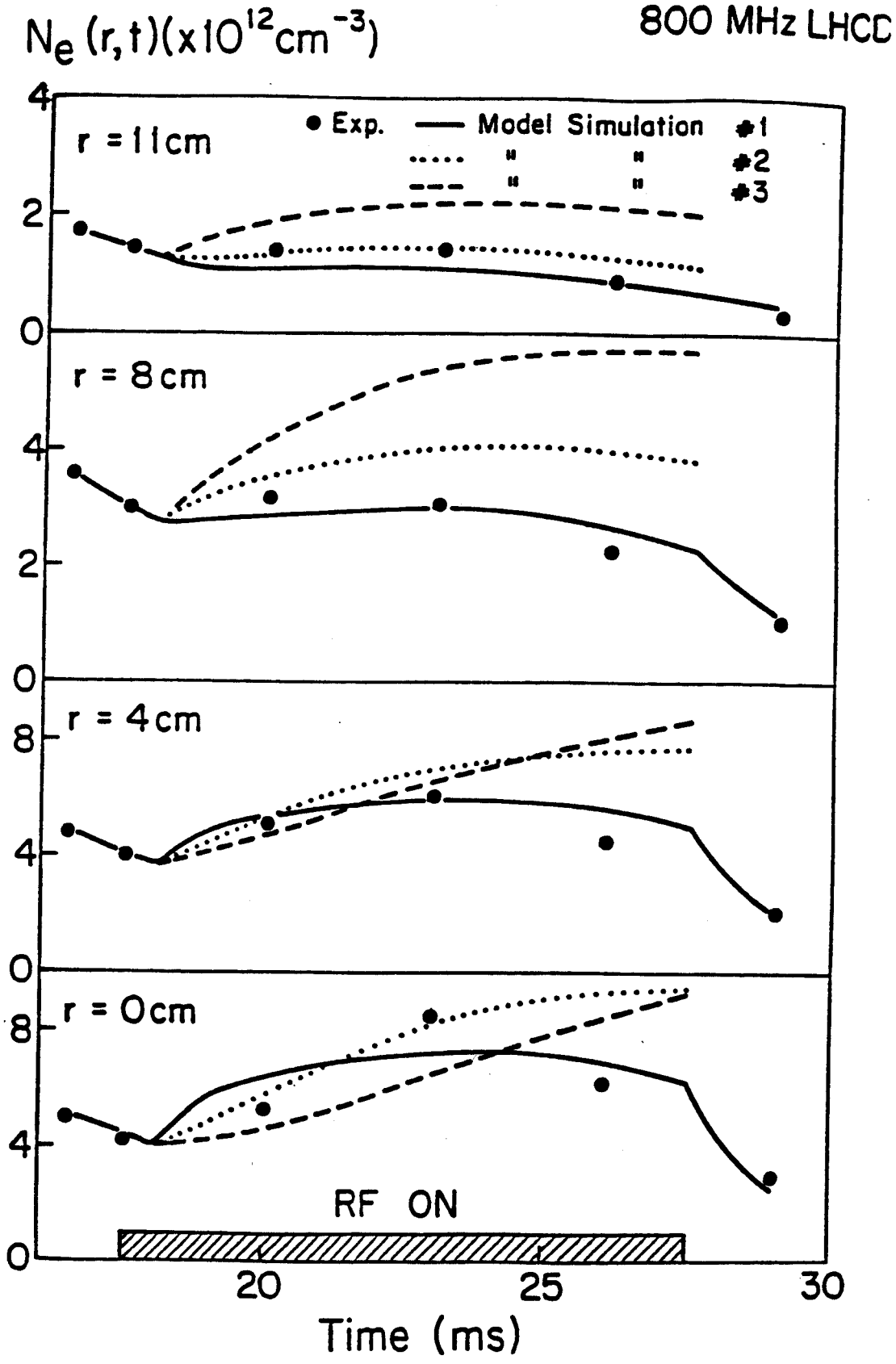
$N_e(r,t)(x10^{12}cm^{-3})$
800 MHz LHCD
Exp.
Model Simulation
#1
#2
#3
r = 11cm
r = 8cm
r = 4cm
r = 0cm
RF ON
Time (ms)

Fig. 3

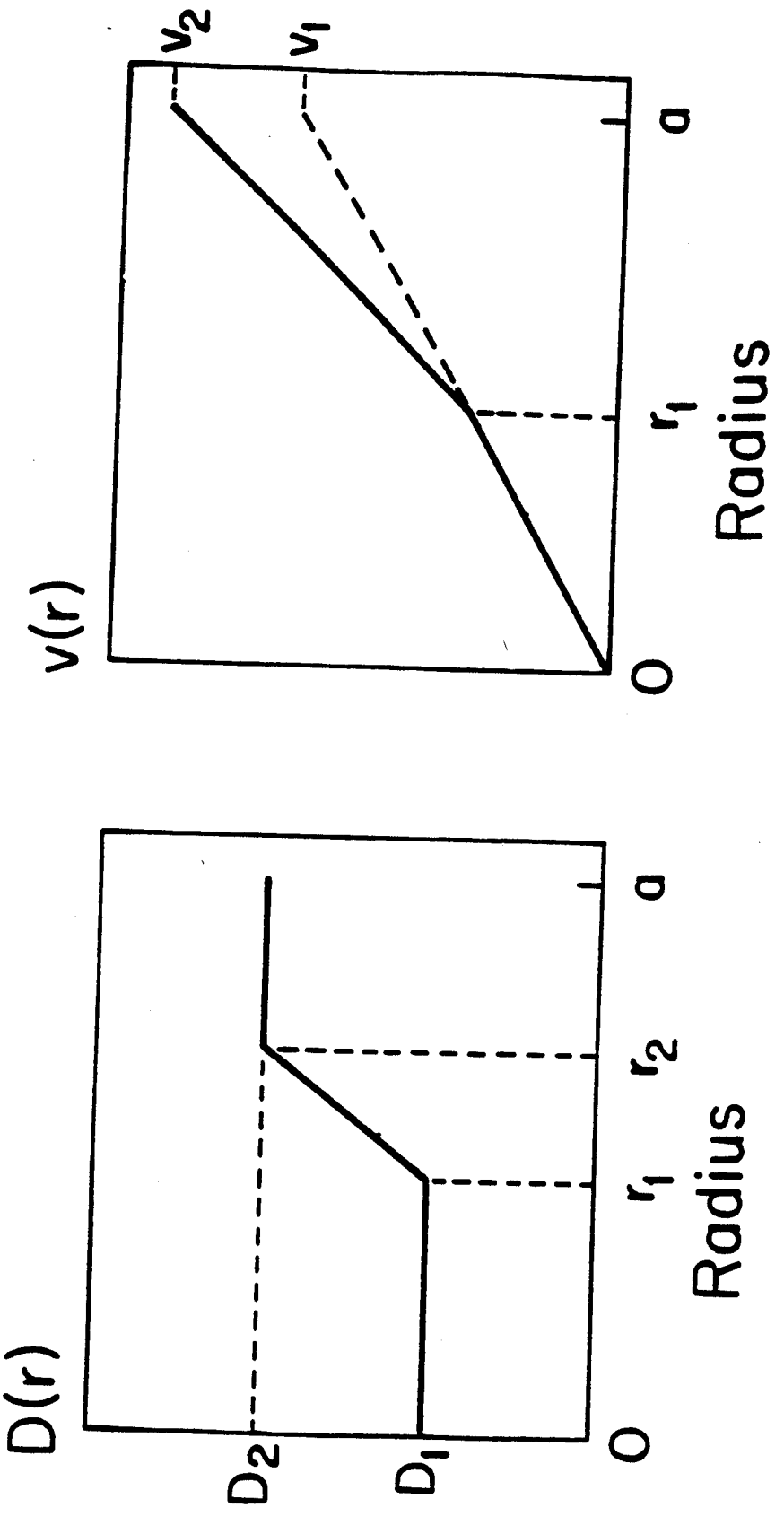

Fig. 4

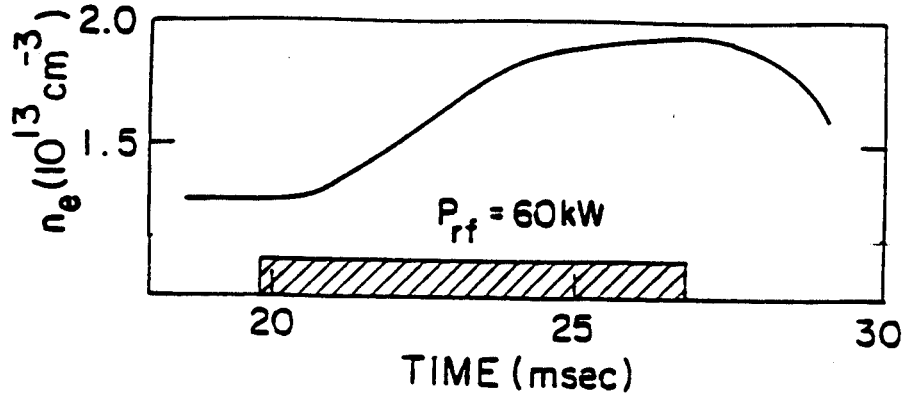
$n_e(10^{13}cm^{-3})$
2.0
1.5
P_{rf} = 60kW
20
25
30
TIME (msec)

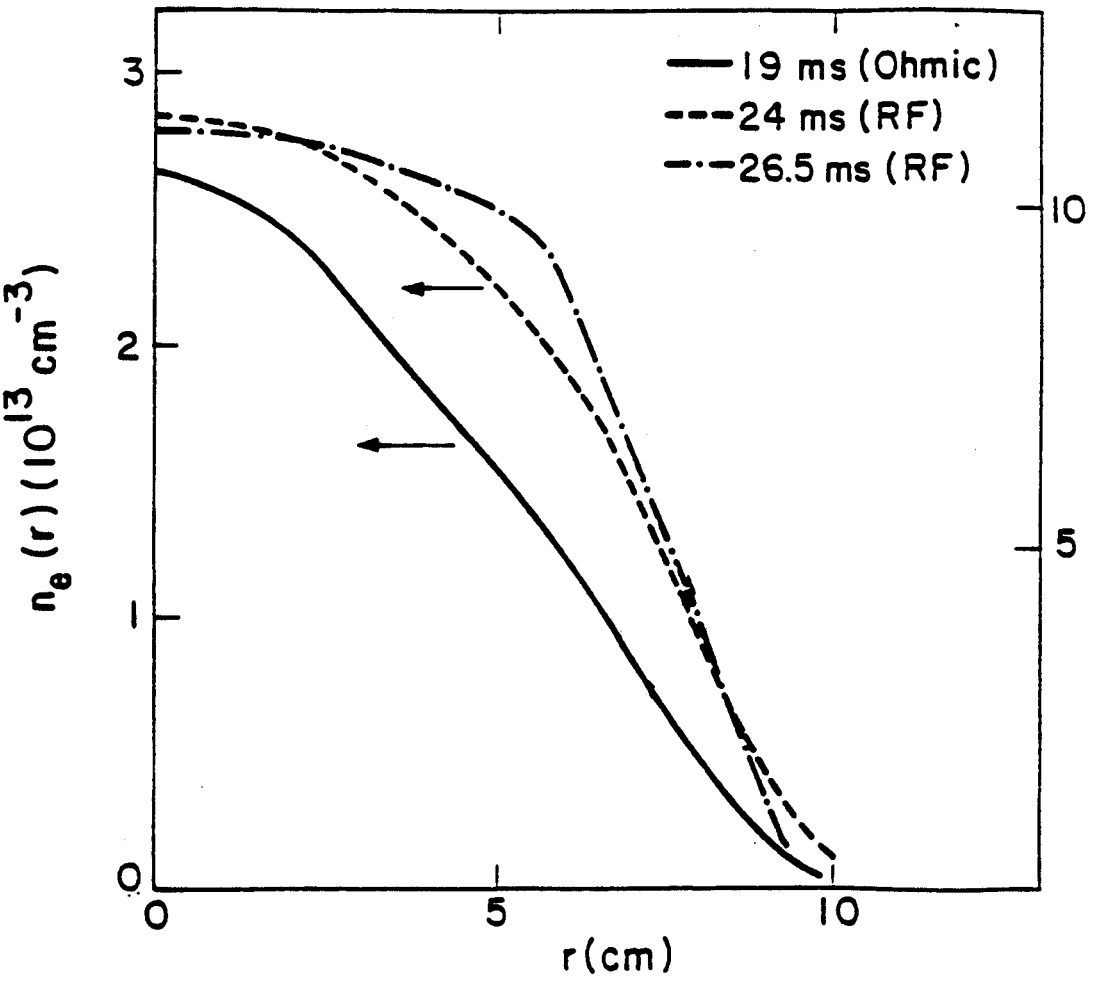
19 ms (Ohmic)
24 ms (RF)
26.5 ms (RF)
$n_e(r)(10^{13}cm^{-3})$
3
2
1
0
10
5
0
5
10
r(cm)

Fig. 5

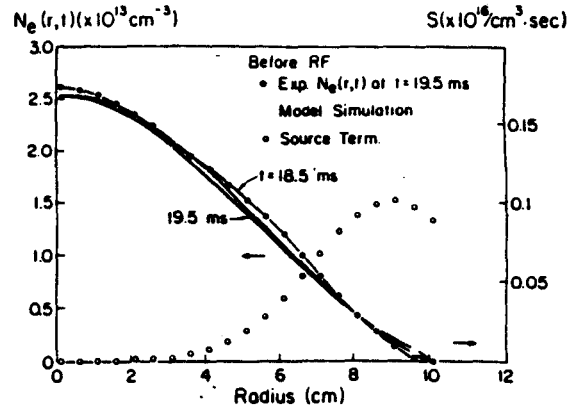
N_e (r,t)(x10^{13}cm^{-3})
S(x10^{16}/cm^3·sec)
Before RF
• Exp. N_e(r,t) at t=19.5 ms
Model Simulation
• Source Term
t=18.5 ms
19.5 ms
Radius (cm)

(a)

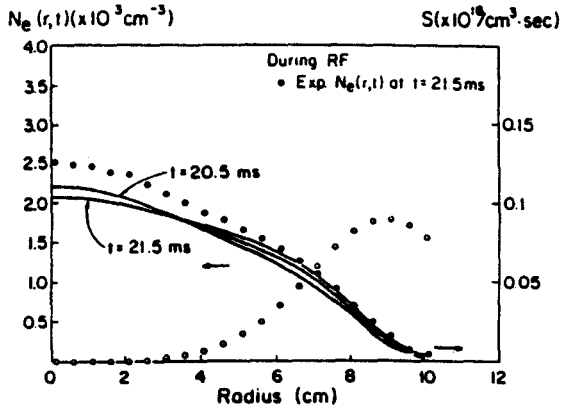
N_e (r,t)(x10^{3}cm^{-3})
S(x10^{16}/cm^3·sec)
During RF
• Exp. N_e(r,t) at t=21.5ms
t=20.5 ms
t=21.5 ms
Radius (cm)

(b)

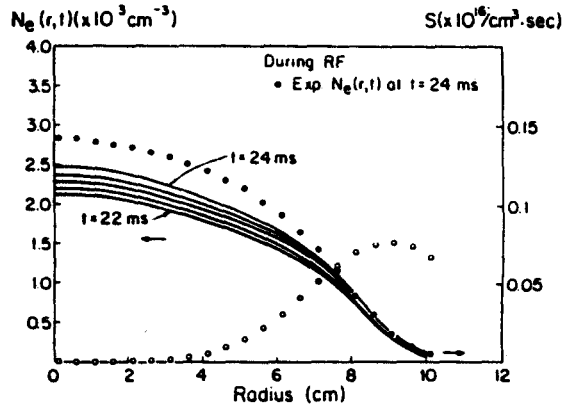
N_e (r,t)(x10^{3}cm^{-3})
S(x10^{16}/cm^3·sec)
During RF
• Exp. N_e(r,t) at t=24 ms
t=24 ms
t=22 ms
Radius (cm)

(c)

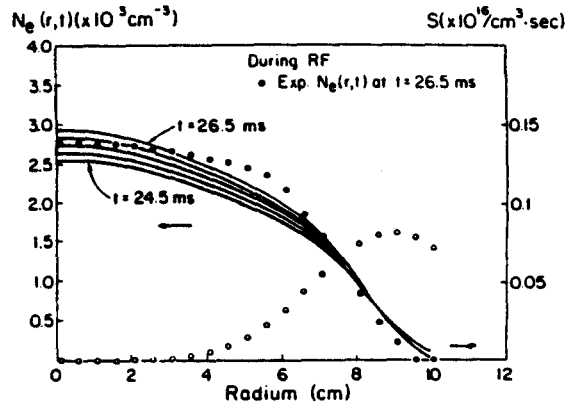
N_e (r,t)(x10^{3}cm^{-3})
S(x10^{16}/cm^3·sec)
During RF
• Exp. N_e(r,t) at t=26.5 ms
t=26.5 ms
t=24.5 ms
Radium (cm)

(d)

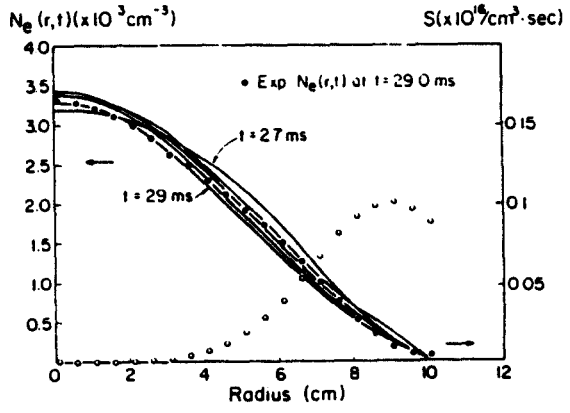
N_e (r,t)(x10^{3}cm^{-3})
S(x10^{16}/cm^3·sec)
• Exp. N_e(r,t) at t=29.0 ms
t=27 ms
t=29 ms
Radius (cm)

(e)

Fig. 6

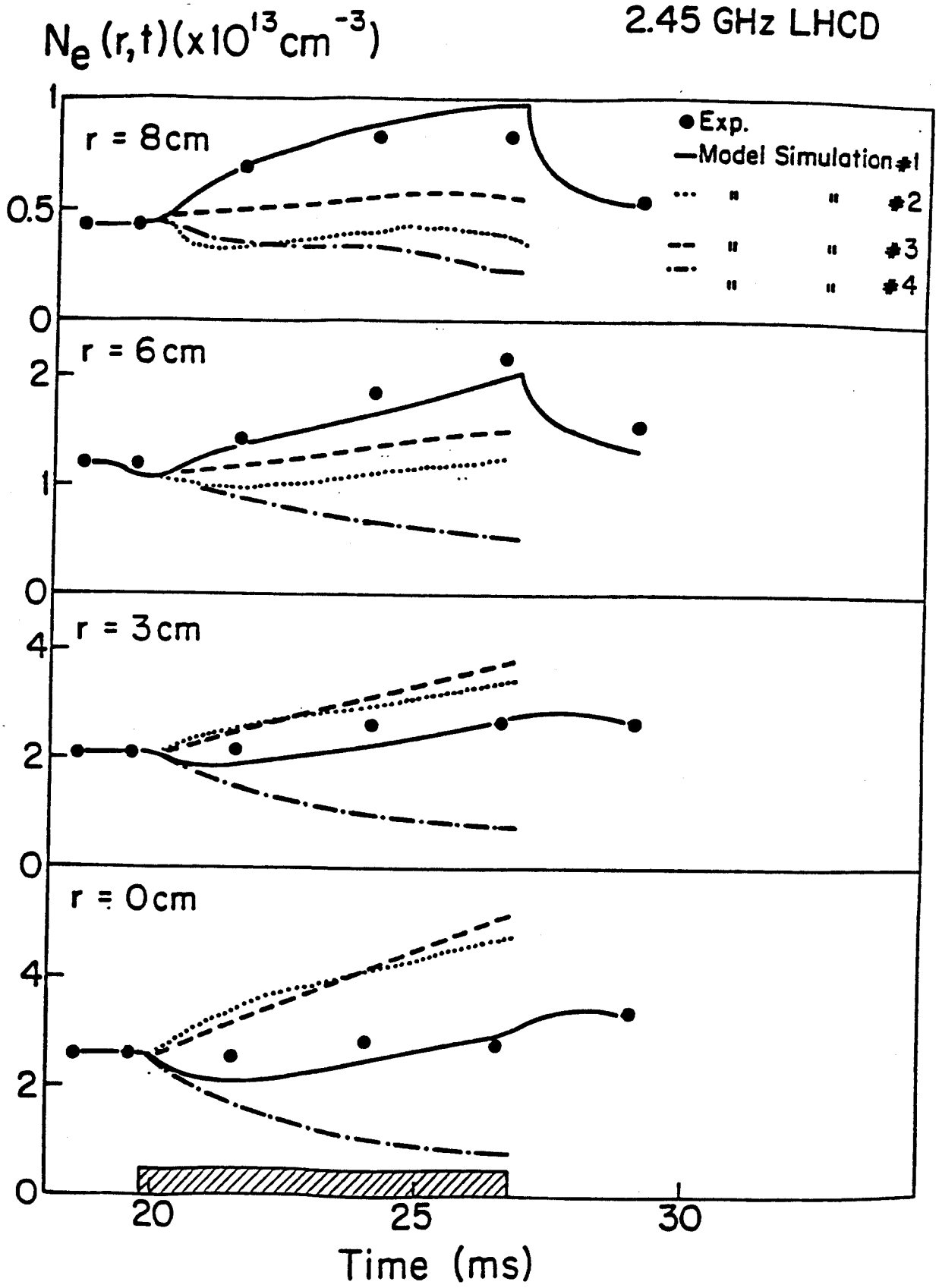
N_e (r,t)(x10^{13}cm^{-3})
2.45 GHz LHCD
r = 8cm
r = 6cm
r = 3cm
r = 0cm
●Exp.
—Model Simulation #1
··· " " #2
-- " " #3
-·- " " #4
1
0.5
0
2
1
0
4
2
0
4
2
0
20
25
30
Time (ms)

Fig. 7

800 MHz LHCD

Before RF		During RF			After RF	
$D(\times 10^3 cm^2/sec)$	$v(\times 10^3 cm^2/sec)$		$D(\times 10^3 cm^2/sec)$	$v(\times 10^3 cm^2/sec)$	$D(\times 10^3 cm^2/sec)$	$v(\times 10^3 cm/sec)$
15	$0.6 \times \frac{r}{a}$	Model Simulation #1	15	$5.2 \times \frac{r}{a}$	$D_1 = 15$ $D_2 = 25$ $r_1 = 5cm$ $r_2 = 10cm$	$0.6 \times \frac{r}{a}$
		Model Simulation #2	6	$2 \times \frac{r}{a}$		
		Model Simulation #3	2	$0.6 \times \frac{r}{a}$		

Table I

2.45 GHz LHCD

Before RF		During RF			After RF	
$D(\times 10^3 cm^2/sec)$	$v(\times 10^3 cm^2/sec)$		$D(\times 10^3 cm^2/sec)$	$v(\times 10^3 cm^2/sec)$	$D(\times 10^3 cm^2/sec)$	$v(\times 10^3 cm/sec)$
5	$2.1 \times \frac{r}{a}$	Model Simulation #1	$D_1 = 8$ $D_2 = 2$ $r_1 = 5$ cm $r_2 = 8$ cm	$2.1 \times \frac{r}{a}$	5	$2.1 \times \frac{r}{a}$
		Model Simulation #2	5	$4.2 \times \frac{r}{a}$		
		Model Simulation #3	2.5	$2.1 \times \frac{r}{a}$		
		Model Simulation #4	5	$v_1 = 0.5$ $v_2 = 4.2$ $r_1 = 3$ cm		

Table II

800 MHz LHCD

Time (ms)	Radius (cm)	v/D (cm^{-1})	
		from profile measurement	from model
17.5	5	0.025	0.016
23	5	0.14	0.135

2.45 GHz LHCD

Time (ms)	Radius (cm)	v/D (cm^{-1})	
		from profile measurement	from model
19.5	4	0.154	0.17
26.5	4	0.04	0.10

Table III